



Two lanthanide–sodium pillared-layer frameworks constructed from 4,4'-oxybis(benzoic acid) and oxalate

Jing Xu, Weiping Su*, Maochun Hong

State Key Laboratory of Structural Chemistry, Fujian Institute of Research on the Structure of Matter, Chinese Academy of Sciences, Fuzhou, Fujian 350002, PR China

ARTICLE INFO

Article history:

Received 11 July 2011

Accepted 16 August 2011

Available online 25 August 2011

Keywords:

Lanthanide(III)–sodium(I)

Pillared-layer frameworks

Hydrothermal reaction

Anti-ferromagnetic property

ABSTRACT

Two new heterometallic lanthanide(III)–sodium(I) coordination polymers [LnNa(4,4'-oba)(ox)(H₂O)] (Ln = Nd **1**, Sm **2**) have been synthesized by hydrothermal reactions of 4,4'-Oxybis(benzoic acid) (4,4'-H₂oba) and Na₂C₂O₄ with corresponding lanthanide nitrate. Both compounds are isostructural and possess three-dimensional (3D) pillared-layer frameworks comprising Ln–Na–oxalate layers and 4,4'-oba pillars. The magnetic properties reveal that the two compounds have anti-ferromagnetic behaviors. Furthermore, the IR, PXRD, elemental and TG analyses are also investigated.

© 2011 Elsevier B.V. All rights reserved.

The design and construction of metal–organic frameworks (MOFs) have provoked increasing interest not only from their fascinating topological networks [1] but also from their potential applications in gas storage and separation [2], magnetism [3], luminescence [4], and catalysis [5]. To design and construct MOFs, the reasonable selection of metal ion and organic ligand is very important. Recently, lanthanides as metal centers, with high coordination number and variable coordination environments [6] together with the special luminescent [4b] and magnetic [3a,4a] properties deriving from 4f electrons, have drawn considerable attention. As is well known, Ln ions have high affinity and prefer to bind to oxygen donor atoms, thus polycarboxylate ligands, such as pyridinecarboxylate [7], imidazolecarboxylate [8], and benzenepolycarboxylate [9], have been widely employed in the construction of lanthanide-based MOFs (LnMOFs). Furthermore, due to the potential applications of pillared-layer MOFs in adsorption, separation and catalysis [10], it is necessary to further research the construction of pillared-layer MOFs.

Up to now, much work is centered on using one type of ligand. If an auxiliary ligand was to be introduced, the cooperativity of both ligands may offer possibilities for the formation of unforeseen LnMOFs with useful properties [11]. Inspired by our previous experience [12], in this contribution, we chose two types of 4,4'-Oxybis(benzoic acid) (4,4'-H₂oba) and oxalate as mixed ligands to construct lanthanide coordination frameworks, based on the following considerations: (1) 4,4'-H₂oba, as a V-shaped, flexible and long spacer with two carboxylate groups, shows versatile coordination modes, which makes it a useful

bridge to construct coordination polymers [13]; (2) oxalate, as one of the simplest bis-bidentate connectors, can facilitate the formation of extended structures by bridging metal centers [14]. Accordingly, our aim is to synthesize new LnMOFs based on mixed ligands with useful properties.

Herein, we report the syntheses and characterization of two new isostructural 3D Ln–Na pillared-layer coordination polymers: [LnNa(4,4'-oba)(ox)(H₂O)] (Ln = Nd **1**, Sm **2**), in which 4,4'-oba ligands work as pillars and link the Ln–Na–oxalate layers, resulting in pillared-layer heterometallic frameworks. The as-synthesized samples of two compounds have also been measured by IR, PXRD, elemental and TG analyses.

Compounds **1** and **2** were successfully synthesized in the same conditions by the hydrothermal reactions of Ln(NO₃)₃ (Ln = Nd, Sm), 4,4'-H₂oba and Na₂C₂O₄ in a molar ratio of 1:1:2 at 170 °C [15]. X-ray structural analyses [16] reveal that compounds **1** and **2** are isostructural and crystallize in the monoclinic *P*2₁/*c* space group. Therefore, only the crystal structure of **1** is described in detail. The selected bond lengths and angles are given in Table S1. The hydrogen bond parameters are listed in Table S2.

As shown in Fig. 1, the asymmetric unit of **1** contains one Nd³⁺ ion, one Na⁺ ion, one 4,4'-oba ligand, one oxalate ligand and one coordinated water molecule. Nd atom is nine-coordinated and has distorted tricapped trigonal prism geometry: four O_{COO} atoms from three 4,4'-oba ligands, and five O_{COO} atoms from three oxalate ligands (Fig. S2). The Nd–O bond lengths vary from 2.395(3) to 2.545(3) Å and the O–Nd–O angles range from 64.37(9) to 103.50(11)° (Table S1). Owing to the effect of lanthanide contraction, the Sm–O bond lengths in **2** are slightly shorter than the corresponding Nd–O bond lengths in **1** (Table S1). Na atom is six-coordinated and surrounded by three O_{COO} atoms from three oxalate ligands, two O_{COO} atoms from

* Corresponding author. Tel./fax: +86 591 8377 1575.
E-mail address: wpsu@fjirsm.ac.cn (W. Su).

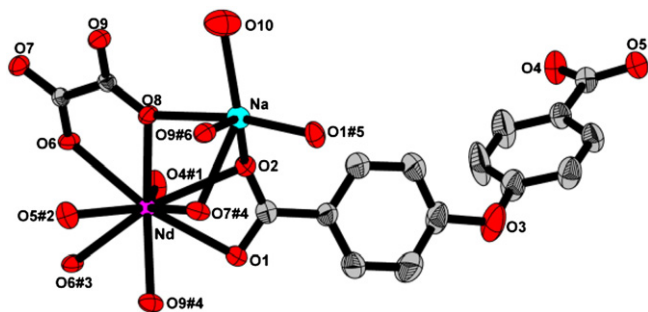


Fig. 1. The asymmetric unit of **1** with 30% thermal ellipsoids. All hydrogen atoms are omitted for clarity. Symmetry codes for the generated atoms are the same as Table S1.

two 4,4'-oba ligands and one coordinated water molecule, exhibiting a distorted octahedral geometry (Fig. S3), with the Na—O bond lengths being 2.291(4)–2.719(4) Å and the O—Na—O angles being 70.33(11)–112.40(13)° (Table S1).

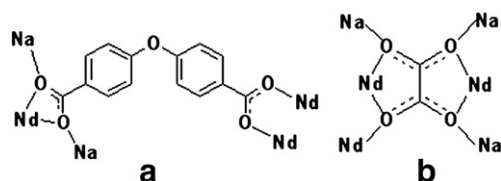
Owing to the high cooperativity between 4,4'-oba and oxalate ligands, the 4,4'-oba ligand only adopts a single $\mu_6-\eta^2, \eta^2, \eta^1, \eta^1$ coordination mode by connecting two Na⁺ ions and three Nd³⁺ ions (Scheme 1a) and the oxalate ligand links three Na⁺ ions and three Nd³⁺ ions adopting a single $\mu_8-\eta^2, \eta^2, \eta^2, \eta^2$ coordination mode (Scheme 1b). As shown in Fig. 2a, Nd and its neighboring Nd (symmetry #3: 2 - x, -y, -z) are linked together through two μ_2 -O atoms of two oxalate ligands to form an edge-sharing metallic dimer with a Nd··Nd distance about 4.079(2) Å.

The Nd₂ dimer further connects two neighboring Na atoms through six O_{COO} atoms forming a {Nd₂Na₂} second building units (SBUs), in which the Nd··Na distance is 3.672(3) Å. Then the oxalate ligands bridge these {Nd₂Na₂} SBUs into two dimensional (2D) heterometallic layers in the bc plane (Fig. 2b). Finally, 4,4'-oba ligands act as pillars to link the Ln–Na–oxalate layers into a 3D pillared-layer network along the b axis (Fig. 3). PLATON calculated a total potential solvent-accessible volume of about 86.4 Å³ (approximately 4.7% of unit cell).

The synthesized products of compounds **1** and **2** have been characterized by powder X-ray diffraction (PXRD) (Fig. S4). The experimental PXRD patterns correspond well with the results simulated from the single crystal data, indicating the high purity of the synthesized samples. The difference in reflection intensities between the simulated and experimental patterns was due to the variation in preferred orientation of the powder samples during the collection of the experimental PXRD data.

The thermal stabilities of **1** and **2** were examined by the thermogravimetric analysis (TGA) in N₂ atmosphere with a heating rate of 15 °C/min from 30 to 1000 °C. These two compounds both undergo two steps of weight loss (Fig. S5). TG curves of **1** and **2** show that from 90 to 285 °C one coordinated water molecule was gradually lost for **1** (calcd/found: 3.4/3.8%), and for **2** (calcd/found: 3.36/3.79%), respectively. Above 420 °C, the frameworks began to collapse accompanying with the decomposition of the organic ligands.

Temperature dependence of magnetic susceptibilities of compounds **1** and **2** have been performed on the polycrystalline samples in the temperature range 2–300 K. The plots of $\chi_M T$ and χ_M vs. *T* for compounds **1**



Scheme 1. Coordination modes of the 4,4'-oba and oxalate ligands observed in **1**.

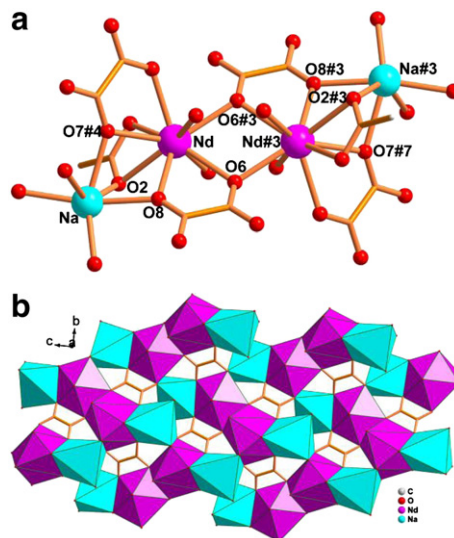


Fig. 2. (a) View of {Nd₂Na₂} SBUs in **1**. Symmetry codes for the generated atoms (except O7#7: x, -0.5 - y, -0.5 + z) are the same as Table S1. (b) The 2D layer with Nd(III)–Na(I) bridged by oxalate.

and **2** are given in Fig. 4. As shown in Fig. 4a, at 300 K, the experimental $\chi_M T$ value of **1** is 1.63 cm³ K mol⁻¹, which is close to the expected value of 1.64 cm³ K mol⁻¹ for one single Nd³⁺ ion with a ⁴I_{9/2} ground state [3a]. As the temperature is lowered, $\chi_M T$ decreases to a minimum at about 4.5 K and then increases rapidly to reach 0.72 cm³ K mol⁻¹ at 2 K. The plot of χ_M^{-1} vs. *T* over the temperature range 30–300 K obeys the Curie–Weiss law [$\chi_M = C/(T - \theta)$] with $C = 1.92$ cm³ K mol⁻¹ and $\theta = -67.99$ K. The decrease of $\chi_M T$ and the negative value of θ may be due to the depopulations of the Stark levels and/or possible anti-ferromagnetic interactions between Nd³⁺ ions [17], and the increase at low temperature reveals dominant ferromagnetic interaction between Nd³⁺ ions. As shown in Fig. 4b, for **2**, the observed $\chi_M T$ value is 0.48 cm³ K mol⁻¹, which is slightly higher than the expected value of 0.32 cm³ K mol⁻¹ for one single Sm³⁺ ion. As the temperature cools down, the $\chi_M T$ value monotonously decreases, which is obviously attributed to the thermal depopulation of the stark component of lanthanide ion at low temperature [3a,18]. At 2 K, $\chi_M T$ is 0.03 cm³ K mol⁻¹, which is slightly lower than the expected value of 0.09 cm³ K mol⁻¹ for one Sm³⁺ ion with a ⁶H_{5/2} ground state [3a]. The decrease of $\chi_M T$ value on cooling indicates the anti-ferromagnetic interactions between Sm³⁺ ions within **2**.

In summary, we have successfully synthesized two 3D Ln(III)–Na(I) heterometallic coordination polymers, each with a pillared-layer network based on Ln–Na–oxalate layers pillared by 4,4'-oba ligands. Both compounds show anti-ferromagnetic properties. This work opens new

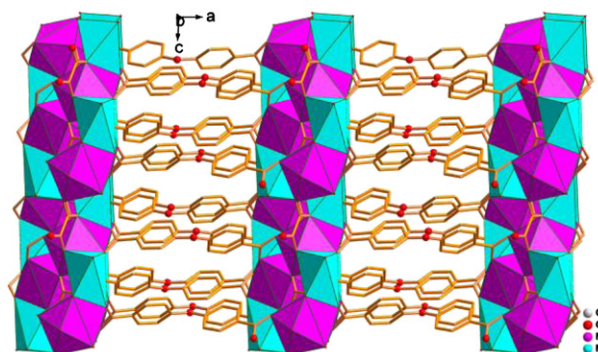


Fig. 3. View of the 3D pillared-layer network along the *b* axis for **1**.

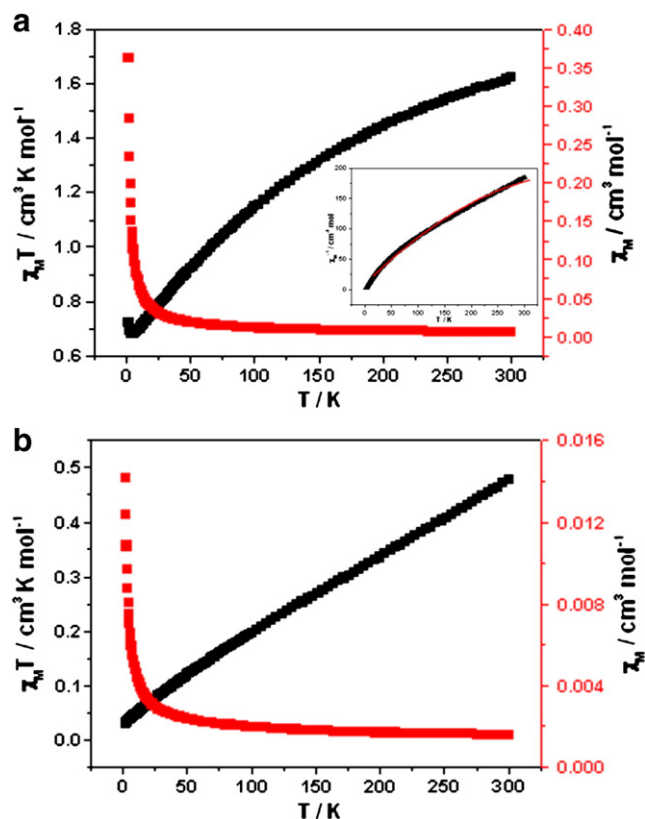


Fig. 4. (a) Temperature dependence of $\chi_M T$, χ_M , and χ_M^{-1} (inset) for **1** at 1 KOe. (b) Temperature dependence of $\chi_M T$ and χ_M for **2** at 1 KOe.

perspectives and a rational route to construct heterometallic pillared-layer frameworks.

Acknowledgments

This work is financially supported by 973 Program (2011CB932404, 2011CBA00501), NSFC (20821061, 20925102), “The Distinguished Oversea Scholar Project”, “One Hundred Talent Project”, and Key Project from CAS.

Appendix A. Supplementary data

X-ray crystallographic data for compounds **1** and **2** in cif format, general characterizations (IR, PXRD and TGA), crystallographic data and additional structure figures. Supplementary data to this article can be found online at doi:10.1016/j.inoche.2011.08.012.

References

- (a) B. Moulton, M.J. Zaworotko, From molecules to crystal engineering: supramolecular isomerism and polymorphism in network solids, *Chemical Reviews* 101 (2001) 1629–1658;
- (b) J.F. Stoddart, The master of chemical topology, *Chemical Society Reviews* 38 (2009) 1521–1529;
- (c) D.B. Amabilino, L. Pérez-García, Topology in molecules inspired, seen and represented, *Chemical Society Reviews* 38 (2009) 1562–1571.
- (a) M. Eddaoudi, J. Kim, N. Rosi, D. Vodak, J. Wachter, M. O’Keeffe, O.M. Yaghi, Systematic design of pore size and functionality in isoreticular MOFs and their application in methane storage, *Science* 295 (2002) 469–472;
- (b) L. Pan, B. Parker, X. Huang, D.H. Olson, J.Y. Lee, J. Li, Zn(tbip) ($\text{H}_2\text{tbip} = 5\text{-tert-Butyl isophthalic acid}$): a highly stable guest-free microporous metal organic framework with unique gas separation capability, *Journal of the American Chemical Society* 128 (2006) 4180–4181;
- (c) M. Xue, Z. Zhang, S. Xiang, Z. Jin, C. Liang, G.S. Zhu, S.L. Qiu, B.L. Chen, Selective gas adsorption within a five-connected porous metal–organic framework, *Journal of Materials Chemistry* 20 (2010) 3984–3988;
- (d) D. Zhao, D.J. Timmons, D. Yuan, H.C. Zhou, Tuning the topology and functionality of metal–organic frameworks by ligand design, *Accounts of Chemical Research* 44 (2011) 123–133;
- (e) S.S. Chen, M. Chen, S. Takamizawa, P. Wang, G.C. Lv, W.Y. Sun, Porous cobalt (II)-imidazolate supramolecular isomeric frameworks with selective gas sorption, *Chemical Communications* 47 (2011) 4902–4904.
- (a) C. Benelli, D. Gatteschi, Magnetism of lanthanides in molecular materials with transition-metal ions and organic radicals, *Chemical Reviews* 102 (2002) 2369–2387;
- (b) D. Maspocho, D. Ruiz-Molina, J. Veciana, Old materials with new tricks: multifunctional open-framework materials, *Chemical Society Reviews* 36 (2007) 770–818.
- (a) K. Kuriki, Y. Koike, Y. Okamoto, Plastic optical fiber lasers and amplifiers containing lanthanide complexes, *Chemical Reviews* 102 (2002) 2347–2356;
- (b) J.C.G. Bünzli, C. Piguet, Taking advantage of luminescent lanthanide ions, *Chemical Society Reviews* 34 (2005) 1048–1077.
- (a) M. Shibusaki, N. Yoshikawa, Lanthanide complexes in multifunctional asymmetric catalysis, *Chemical Reviews* 102 (2002) 2187–2209;
- (b) J. Inanaga, H. Furuno, T. Hayano, Asymmetric catalysis and amplification with chiral lanthanide complexes, *Chemical Reviews* 102 (2002) 2211–2225.
- J.C.G. Bünzli, C. Piguet, Lanthanide-containing molecular and supramolecular polymeric functional assemblies, *Chemical Reviews* 102 (2002) 1897–1928.
- (a) P. Mahata, K.V. Ramya, S. Natarajan, Pillaring of CdCl_2 -like layers in lanthanide metal–organic frameworks: synthesis, structure, and photo-physical properties, *Chemistry – A European Journal* 14 (2008) 5839–5850;
- (b) M.S. Liu, Q.Y. Yu, Y.P. Cai, C.Y. Su, X.M. Lin, X.X. Zhou, J.W. Cai, One-, two-, and three-dimensional lanthanide complexes constructed from pyridine-2,6-dicarboxylic acid and oxalic acid ligands, *Crystal Growth and Design* 8 (2008) 4083–4091;
- (c) J. Xu, W. Su, M. Hong, A series of lanthanide secondary building units based metal–organic frameworks constructed by organic pyridine-2,6-dicarboxylate and inorganic sulfate, *Crystal Growth and Design* 11 (2011) 337–346.
- (a) Y.Q. Sun, J. Zhang, Y.M. Chen, G.Y. Yang, Porous lanthanide–organic open frameworks with helical tubes constructed from interweaving triple-helical and double-helical chains, *Angewandte Chemie, International Edition* 44 (2005) 5814–5817;
- (b) Z.X. Wang, Q.F. Wu, H.J. Liu, M. Shao, H.P. Xiao, M.X. Li, 2D and 3D lanthanide coordination polymers constructed from benzimidazole-5,6-dicarboxylic acid and sulfate bridged secondary building units, *Crystal Engineering Communications* 12 (2010) 1139–1146.
- (a) R. Cao, D. Sun, Y. Liang, M. Hong, K. Tatsumi, Q. Shi, Syntheses and characterizations of three-dimensional channel-like polymeric lanthanide complexes constructed by 1,2,4,5-benzenetetracarboxylic acid, *Inorganic Chemistry* 41 (2002) 2087–2094;
- (b) X. Guo, G. Zhu, F. Sun, Z. Li, X. Zhao, X. Li, H. Wang, S. Qiu, Synthesis, structure, and luminescent properties of microporous lanthanide metal–organic frameworks with inorganic rod-shaped building units, *Inorganic Chemistry* 45 (2006) 2581–2587.
- M. Eddaoudi, D.B. Moler, H. Li, B. Chen, T.M. Reineke, M. O’Keeffe, O.M. Yaghi, Modular chemistry: secondary building units as a basis for the design of highly porous and robust metal–organic carboxylate frameworks, *Accounts of Chemical Research* 34 (2001) 319–330.
- J.W. Cheng, J. Zhang, S.T. Zheng, M.B. Zhang, G.Y. Yang, Lanthanide–transition-metal sandwich framework comprising (Cu_3) cluster pillars and layered networks of $\{\text{Er}_{36}\}$ wheels, *Angewandte Chemie, International Edition* 45 (2006) 73–77.
- J. Xu, J. Cheng, W. Su, M. Hong, Effect of lanthanide contraction on crystal structures of three-dimensional lanthanide based metal–organic frameworks with thiophene-2,5-dicarboxylate and oxalate, *Crystal Growth and Design* 11 (2011) 2294–2301.
- C.Y. Sun, S. Gao, L.P. Jin, Hydrothermal syntheses, architectures and magnetic properties of six novel Mn^{II} coordination polymers with mixed ligands, *European Journal of Inorganic Chemistry* (2006) 2411–2421.
- C.N.R. Rao, S. Natarajan, R. Vaidyanathan, Metal carboxylates with open architectures, *Angewandte Chemie, International Edition* 43 (2004) 1466–1496.
- Synthesis of compound **1**: A mixture of $\text{Nd}(\text{NO}_3)_3 \cdot 5\text{H}_2\text{O}$ (0.25 mmol, 0.0826 g), 4,4’- $\text{H}_2\text{o}ba$ (0.25 mmol, 0.0646 g), $\text{Na}_2\text{C}_2\text{O}_4$ (0.5 mmol, 0.0670 g), and H_2O (6 mL) was sealed in a 25 mL Teflon-lined autoclave at 170 °C for 4 days, then cooled to room temperature. Pink prismatic crystals of **1** were obtained (yield: 45% based on $\text{Nd}(\text{NO}_3)_3 \cdot 5\text{H}_2\text{O}$). Anal. calc. for $\text{C}_{16}\text{H}_{10}\text{NaNO}_{10}$ (529.47): C, 36.29; H, 1.90%; found: C, 36.42; H, 1.94%. IR spectrum (KBr pellet, ν/cm^{-1}): 3542.8(m), 3460(m), 1697.3(s), 1640.1(s), 1598.8(vs), 1540.8(s), 1425.8(s), 1384.4(vs), 1326.5(m), 1244.5(s), 1161.8(s), 1096.4(vw), 1005.4(vw), 873.8(m), 799.3(s), 700.8(m), 659.4(m), 626.3(w), 560.9(w), 503(m) (left in Fig. S1). Compound **2** was synthesized by a procedure similar to that of **1**, except $\text{Sm}(\text{NO}_3)_3 \cdot 6\text{H}_2\text{O}$ (0.25 mmol, 0.1111 g) replaced $\text{Nd}(\text{NO}_3)_3 \cdot 5\text{H}_2\text{O}$. Pale-yellow prismatic crystals of **2** were obtained (yield: 50% based on $\text{Sm}(\text{NO}_3)_3 \cdot 6\text{H}_2\text{O}$). Anal. calc. for $\text{C}_{16}\text{H}_{10}\text{NaSmO}_{10}$ (535.58): C, 35.88; H, 1.88%; found: C, 35.65; H, 1.89%. IR spectrum (KBr pellet, ν/cm^{-1}): 3542.8(m), 3460(m), 1697.2(s), 1640(s), 1598.8(vs), 1540.8(s), 1425.8(s), 1384.4(vs), 1326.5(m), 1244.5(s), 1161.8(s), 1096.4(vw), 1005.4(vw), 873.8(m), 799.3(s), 700.8(w), 659.4(m), 626.3(w), 560.9(w), 503(m) (right in Fig. S1).
- Crystal data for **1** ($\text{C}_{16}\text{H}_{10}\text{NaNO}_{10}$): Fw = 529.47, monoclinic, $P2_1/c$, $a = 15.940(3)$ Å, $b = 10.9813(19)$ Å, $c = 10.5913(19)$ Å, $\beta = 93.273(2)^\circ$, $V = 1850.9(6)$ Å³, $Z = 4$, $\rho = 1.900$ g/cm³, $\mu = 2.881$ mm⁻¹, GOF = 1.100. A total of 14193 reflections were collected and 4227 reflections are unique ($R_{\text{int}} = 0.0374$). $R_1/wR_2 = 0.0385/0.0934$ for 254 parameters and 3984 reflections $I > 2\sigma(I)$. Crystal data for **2** ($\text{C}_{16}\text{H}_{10}\text{NaSmO}_{10}$):

Fw=535.58, monoclinic, P2₁/c, a=15.903(5) Å, b=10.933(3) Å, c=10.540(3) Å, $\beta=92.789(4)^\circ$, V=1830.4(9) Å³, Z=4, $\rho=1.943$ g/cm³, $\mu=3.285$ mm⁻¹, GOF=1.055. A total of 14056 reflections were collected and 4162 reflections are unique ($R_{int}=0.0342$). $R_1/wR_2=0.0334/0.0848$ for 254 parameters and 3952 reflections $I>2\sigma(I)$. Data were collected on a SCXmini CCD diffractometer ($\lambda_{MoK\alpha}=0.71073$ Å), T=293(2) K, and refined by full-matrix least-squares refinements on F^2 using all data with SHELXTL-97 programs [19]. All absorption corrections were performed by using the SADABS program. All non-hydrogen atoms were refined anisotropically. CCDC number 797947 for **1**, 798940 for **2**

- [17] H. Hou, G. Li, L. Li, Y. Zhu, X. Meng, Y. Fan, Synthesis, crystal structures, and magnetic properties of three novel ferrocenecarboxylato-bridged lanthanide dimers, *Inorganic Chemistry* 42 (2003) 428–435.
- [18] X. Lin, T. Liu, J. Lin, H. Yang, J. Lü, B. Xu, R. Cao, Syntheses and characterizations of two new pillared-layer coordination polymers constructed from lanthanides and mixed O-donor ligands, *Inorganic Chemistry Communications* 13 (2010) 388–391 (and references therein).
- [19] G.M. Sheldrick, SHELXTL-97, Program for the Solution of Crystal Structures, University of Göttingen, Germany, 1997.